



Adegbenjo, AO, Nsiah-Baafi, E, Olubambi, PA, Potgieter, JH, Shongwe, MB and Ramakokovhu, M (2017) Dependence of Fracture Patterns in Spark Plasma Sintered Irregular Shaped Ti6Al4V Powders on Densification. In: International Conference on Sustainable Materials Processing and Manufacturing, SMPM 2017, 23 January 2017 - 25 January 2017, Kruger National Park, South Africa.

Downloaded from: <https://e-space.mmu.ac.uk/628321/>

Version: Published Version

Publisher: Elsevier

DOI: <https://doi.org/10.1016/j.promfg.2016.12.079>

Usage rights: Creative Commons: Attribution-Noncommercial-No Derivative Works 4.0

Please cite the published version

<https://e-space.mmu.ac.uk>

International Conference on Sustainable Materials Processing and Manufacturing, SMPM 2017,
23-25 January 2017, Kruger National Park

Dependence of Fracture Patterns in Spark Plasma Sintered Irregular Shaped Ti6Al4V Powders on Densification

Adewale Oladapo Adegbenjo^{a,*}, Elsie Nsiah-Baafi^a, Peter Apata Olubambi^b, Johannes Herman Potgieter^c, Mxolisi Brendon Shongwe^a, Mercy Ramakokovhua

^a*Institute for NanoEngineering Research, Department of Chemical, Metallurgical and Materials Engineering, Tshwane University of Technology, Pretoria 0001, South Africa*

^b*Advanced Materials and Electrochemical Technology Research Group, Department of Chemical Engineering Technology, University of Johannesburg, Johannesburg 2006, South Africa*

^c*School of Chemical and Metallurgical Engineering, University of The Witwatersrand, Johannesburg 2000, South Africa*

Abstract

The effect of densification on the fracture behaviour of spark plasma sintered irregular and angular shaped prealloyed Ti6Al4V powders was investigated in this study. Sintering was performed in vacuum at constant heating rate, applied pressure and holding time of 100 °C/min, 50 MPa and 5 min respectively with sintering temperature varied between 650 – 850 °C. Density measurements on sintered samples were according to Archimedes' principle while microstructural evolution and fractographic studies were carried out using a High Resolution Scanning Electron Microscope (HRSEM). Phase identification in sintered samples was achieved by X-ray diffraction (XRD) and Energy Dispersive Spectroscopy (EDS) respectively. Results showed that fracture pattern changed from intergranular to transgranular as densification improved from lower to higher sintering temperature.

© 2017 The Authors. Published by Elsevier B.V. This is an open access article under the CC BY-NC-ND license (<http://creativecommons.org/licenses/by-nc-nd/4.0/>).

Peer-review under responsibility of the organizing committee of SMPM 2017

Keywords: Ti6Al4V alloy; Sintering; Densification; Fracture; Characterization

* Corresponding author. Tel.: +27-844-127-441.
E-mail address: waleeleect@gmail.com

1. Introduction

The unique combinations of mechanical, corrosion resistance and physical properties exhibited by titanium and its alloys have attracted their use in critical and high demanding application areas such as the automobile, aerospace, chemical and energy industries [1, 2]. Among titanium alloys however, Ti6Al4V (Ti64) is the most widely used $\alpha+\beta$ titanium alloy owing to its excellent comprehensive mechanical performance in service and therefore accounts for 45 % of the total titanium production [2-4]. A major setback in the application of titanium alloys is their high affinity for nitrogen and oxygen during processing, thus resulting in compromised ductility properties. Consequently, a need to handle the processing of titanium alloys in controlled, high temperature and vacuum environments arises and becomes unavoidable if the properties of the product will not be compromised by interstitial contaminants, thereby making the processing of these alloys very expensive [5].

To this end, the powder metallurgy process has been generally accepted as a promising and viable route for the production of titanium alloys due to its low cost, versatility and opportunity of having parts produced to a high precision thereby eliminating the cost of machining and material wastages [6, 7]. The spark plasma sintering (SPS) method (a novel, emerging powder metallurgy consolidation technique) is often used for processing of powders into bulk materials. Despite the requirement of high power input in this process as a result of higher heat losses from the use of graphite dies, the method has continued to attract usage in research environments due to its outweighing advantage of sintering powders to full densification in a relatively short time, at lower temperatures, under low vacuum atmosphere, hence, offering the possibility of high heating and fast cooling rates. Thus making the method economical and cost effective, with high energy conservation and efficiency over the conventional sintering methods [8, 9]. This method was chosen in the current study to fabricate Ti64 discs from prealloyed powders at different sintering temperatures so as to investigate the fracture behaviors of the alloys as a function of sintering temperature.

2. Materials and methods

The starting material used in this study is prealloyed 100 mesh particle sized Ti64 powders with irregular and angular shape morphology as supplied by FlowmasterTM shown in Fig. 1. A predetermined amount of the as-received powder was poured in a Ø 30 mm graphite die for each SPS experimental run and sintered under a vacuum atmosphere setting heating rate, holding time and applied pressure constant at 100 °C/min, 5 min and 50 MPa, respectively, while the sintering temperature was varied between 650 – 850 °C. Discs of sintered Ti64 alloys in the dimension Ø 30 mm × 5 mm height were retrieved from the SPS machine model HHPD – 25 FCT Germany. These were cleaned by sand blasting and grinding in succession to remove the adhering graphite papers. Density measurements were carried out according to Archimedes method and the reported values are average of five different measurements taken from each sample. Relative density was calculated as a function of both the experimental and theoretical densities of the sintered samples.

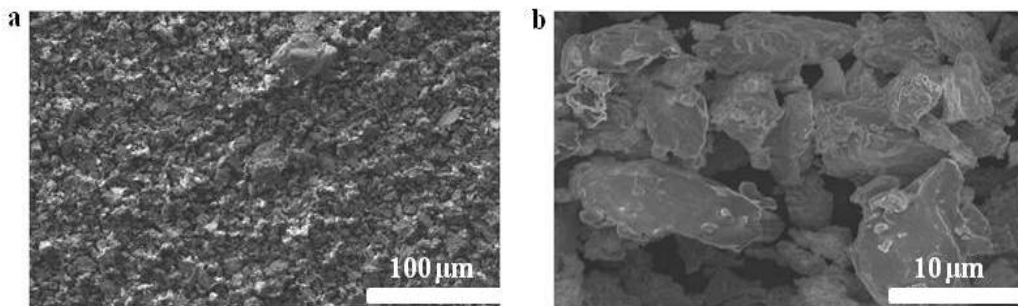


Fig. 1. SEM images of as-received Ti6Al4V powders (a) low magnification; (b) high magnification.

Representative samples from the retrieved alloy discs were prepared for metallographic examinations by the conventional grinding and polishing successions and the mirror finished surfaces were etched with the Kroll solution

(6 mL HF, 12 mLHNO₃ in 150 mL H₂O). Fractographic samples were made by cutting as-sectioned specimens (20 mm × 10 mm × 5 mm) from the sintered alloy discs half way through at the point where the length equals 3:1 (that is, at 15 mm from one end) using a precision cutting machine. This was later clamped to a workbench vise and a hammer was used to tap the 5 mm section to fracture away from the remaining 15 mm length. Microstructural and Fractographic studies of the as-polished and as-fractured sintered specimens respectively were performed using the High Resolution Field Emission Scanning Electron Microscope (JSM-7600F, Jeol, Japan). Phase identification was achieved by Energy Dispersive Spectroscopy and X-Ray Diffraction techniques respectively.

3. Results and discussion

3.1. Densification and microstructural evolution during sintering

Table 1 shows the densification pattern of the sintered prealloyed Ti64 powders as sintering temperature was increased progressively from 650 – 850 °C. It was observed that densification improved with increasing temperature and full densification was attained at 850 °C. The recorded relative densities showed that densification in the sintered alloys were enhanced by 14 % as sintering temperature was increased between 650 and 850 °C. This observation could be explained using the microstructural evolution presented in Fig. 2 as revealed from the Scanning Electron Microscopy studies of the as-etched sintered samples.

Table 1. Densification pattern in sintered Ti64 at different temperatures.

Sintering temperature °C	650	700	750	800	850
Relative density %	85.33	88.04	90.52	95.94	99.55

Fig. 2 (a) shows that the sample sintered at 650 °C was characterized with large and open porosities suggesting that the sample was still far from being sintered and thus justified the observed low relative density. This is in agreement with previous report that the microstructure of sintered Ti64 at lower sintering temperature is inhomogeneous and displays coarse porosity [4]. However, as sintering temperature was increased thereafter from 650 – 850 °C, a progressive pore (seen as black spots) closure was observed. This obviously was responsible for the improvement in densification as the sintering temperature was increased. As full densification was attained at 850 °C, the observed pore sites had closed up almost totally (Fig. 2 (e)) with just only a few pores still identified in the microstructure at this sintering temperature.

Two distinct titanium phases (α and β) usually peculiar to sintered Ti64 alloys were identified from the microstructural evolution (these were also confirmed by the XRD patterns of the sintered powders in Fig. 3), the third ($\alpha+\beta$) being a combination of the former phases. The amount of each phase was seen to be dependent on the sintering temperature and also a function of the dissolved stabilizing element. EDS spot analysis revealed that the α -Ti phase was the dark grey phase, stabilized by dissolved aluminium (Al) and rich in same; while the β -Ti phase seen as a white contrast (indicated by arrow in Fig. 2 (a)) was stabilized by dissolved vanadium (V) and thus is depleted in aluminium.

The $\alpha+\beta$ phase has a widmanstätten (basket weave) structure. This was most prominent at 650 and 750 °C respectively (labeled as point N on the respective micrographs); although, the structure was also observed in Fig. 2 (e) at 850 °C sintering temperature. Thus, the $\alpha+\beta$ widmanstätten structure is presumed to begin forming in the Ti64 alloy used for this present study at a sintering temperature of 650 °C. The structure however grew occupying distinct grains (Fig. 2 (e)) as sintering temperature reached 850 °C. This corroborates the earlier submission of Henriques *et al.* [4] that widmanstätten structure in Ti64 grows with increased sintering temperature and with the dissolution of β stabilizers. The β -phases were mostly on grain boundaries or seen as lath structures within the α -grains. It is worthy of note however that the mechanical properties of the final sintered alloy has a direct correlation with the amount and proportion of the constituting phases.

It also follows from the foregoing that the amount of these phases present in a sintered specimen at a particular sintering temperature as well determines the relative density of the specimen at this chosen temperature as it is

expected that a sample having more of the β -phase will be denser than another one having more of the α -phase as the former is denser than the latter.

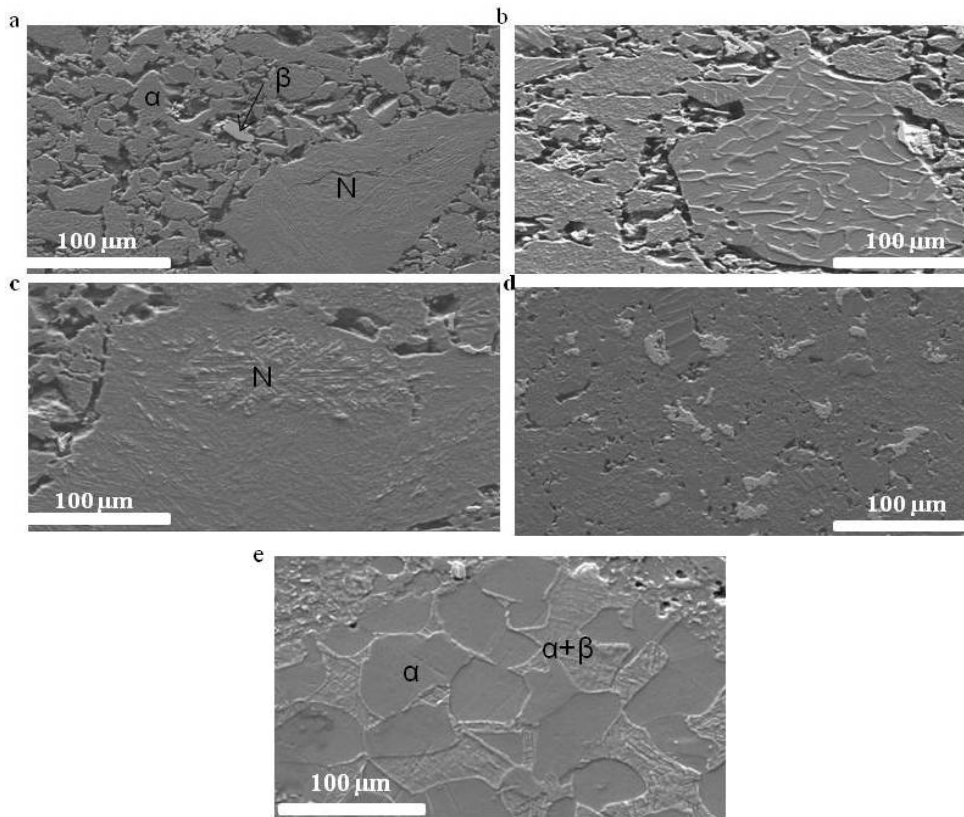


Fig. 2. Microstructural evolution in sintered Ti64 alloy (a) 650 °C; (b) 700 °C; (c) 750 °C; (d) 800 °C; (e) 850 °C.

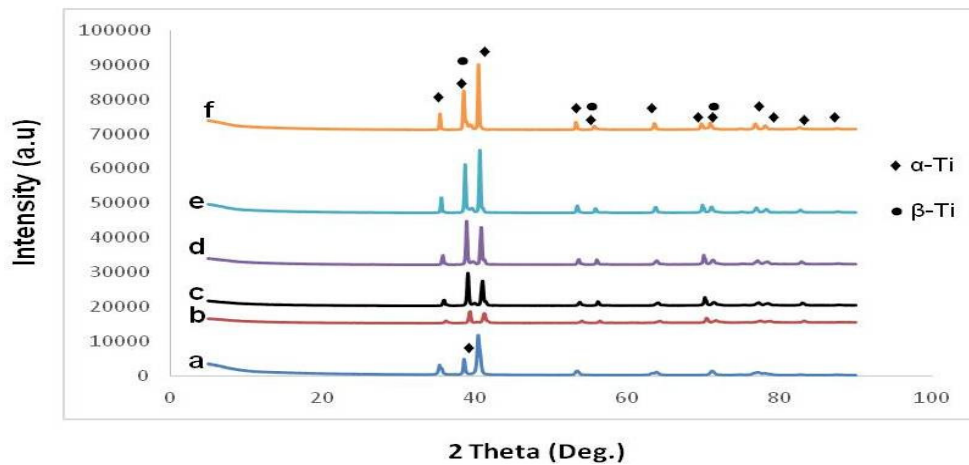


Fig. 3. XRD pattern of (a) as-received Ti64 powder and the sintered Ti64 alloys (b) 650 °C; (c) 700 °C; (d) 750 °C; (e) 800 °C; (f) 850 °C.

3.2. Fracture pattern in sintered Ti64 as a function of densification

The SEM micrographs of the as-fractured surfaces of the sintered Ti64 specimens at different sintering temperatures are presented in Fig. 4. Figs. 4 (a) and (b). It could be seen that there are inherent pores within the fractured surfaces suggesting that the fracture mode in the samples is intergranular and thus a brittle fracture pattern. This was confirmed with the absence of dimples on the fractured surfaces at these sintering temperatures. Also, partially and undeformed particles were observed on the fractured surfaces which is an indication of poor consolidation and that the specimens were not fully sintered.

The fractured surfaces of other samples sintered from 750 – 850 °C (Figs. 4 (c) – (e)) had fine dimples which shows that the fracture mode in these samples is predominantly transgranular thus suggesting that they underwent ductile fracture. The presence of fine dimples also symbolizes good sample cohesion resulting from good sinterability during the SPS processing of the prealloyed Ti64 powders as well as a good strength of the grain boundaries. Fig. 4 (e) presented a plate-like fracture surface morphology which inferentially means that highest deformation of sintered powder particles was achieved at this sintering temperature.

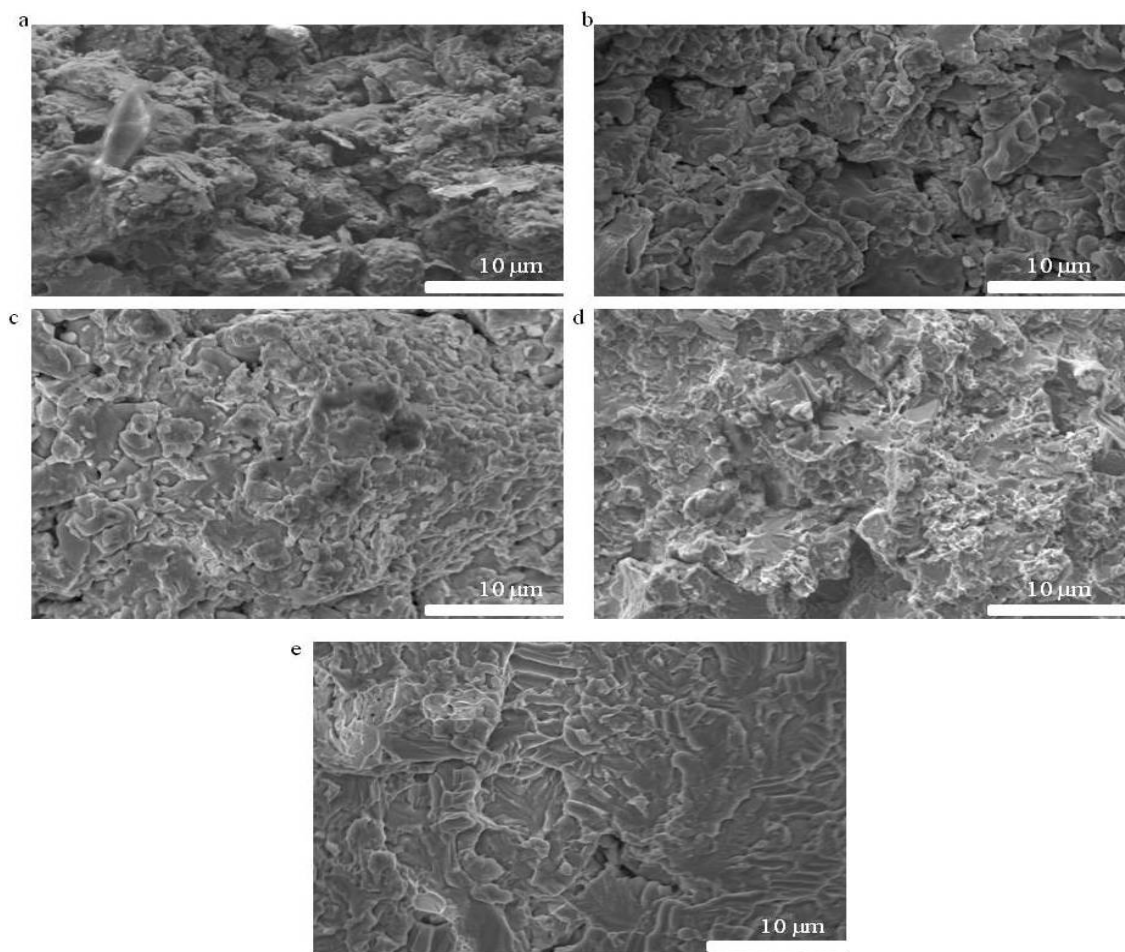


Fig. 4. SEM micrographs of as-fractured surfaces of sintered Ti64 (a) 650 °C; (b) 700 °C; (c) 750 °C; (d) 800 °C; (e) 850 °C.

The fracture surface patterns also showed that deformation of powder particles improved with increased sintering temperature and has a positive correlation with the level of sinterability achieved in the sintered alloy powders. The observed fracture patterns are also directly and well correlated positively with the recorded densification levels for the sintered alloys as presented in Table 1. It then follows that better mechanical properties are expected from the samples with the transgranular fracture mode when put in service.

4. Conclusion

The dependence of the fracture patterns in spark plasma sintered irregular shaped prealloyed Ti6Al4V powders on densification was investigated in this study. The experimental results shows that fracture pattern in the sintered specimens was a transition from intergranular to transgranular as sintering temperature was increased from 650 °C – 850 °C, respectively. It was also concluded that the deformation of powder particles during sintering has a direct correlation with the fracture mode as well as the level of densification and sinterability of the sintered alloy powders.

Acknowledgements

The authors are grateful to Tshwane University of Technology for offering Mr. Adegbenjo a postgraduate bursary award towards his doctoral study and Institute for NanoEngineering Research (INER) for the conducive laboratory environment in support of this research.

References

- [1] S. Chauhan, K. Dass, Dry sliding wear behaviour of titanium (Grade 5) alloy by using response surface methodology, *Advances in Tribology*, 2013 (2013).
- [2] Y. Long, H. Zhang, T. Wang, X. Huang, Y. Li, J. Wu, H. Chen, High-strength Ti–6Al–4V with ultrafine-grained structure fabricated by high energy ball milling and spark plasma sintering, *Materials Science and Engineering: A*, 585 (2013) 408-414.
- [3] A.M. Soufiani, F. Karimzadeh, M. Enayati, Formation mechanism and characterization of nanostructured Ti6Al4V alloy prepared by mechanical alloying, *Materials & Design*, 37 (2012) 152-160.
- [4] V.A.R. Henriques, P.P.d. Campos, C.A.A. Cairo, J.C. Bressiani, Production of titanium alloys for advanced aerospace systems by powder metallurgy, *Materials Research*, 8 (2005) 443-446.
- [5] M. Yan, W. Xu, M. Dargusch, H. Tang, M. Brandt, M. Qian, Review of effect of oxygen on room temperature ductility of titanium and titanium alloys, *Powder Metallurgy*, 57 (2014) 251-257.
- [6] S. Krishnamohan, S. Ramanathan, Synthesis and Characterization of Ti6Al4V Alloy by Powder Metallurgy, *International Journal of Engineering Research and Technology*, ESRSA Publications, 2013.
- [7] F. Froes, D. Eylon, G. Eichelman, H. Burte, Developments in titanium powder metallurgy, *JOM*, 32 (1980) 47-54.
- [8] N. Weston, F. Derguti, A. Tudball, M. Jackson, Spark plasma sintering of commercial and development titanium alloy powders, *Journal of Materials Science*, 50 (2015) 4860-4878.
- [9] F. Zhang, M. Reich, O. Kessler, E. Burkel, The potential of rapid cooling spark plasma sintering for metallic materials, *Materials Today*, 16 (2013) 192-197.